

Nuclear Effects in Semi-inclusive Hadron Production

D. Gaskell (for the HERMES Collaboration)^{a,b}

^aNuclear Physics Laboratory, University of Colorado at Boulder,
UCB 390 , Boulder, CO, 80309, USA

^bJefferson Lab MS 12H, 12000 Jefferson Ave.
Newport News, VA, 23606, USA

Semi-inclusive production of charged hadrons (π^+ , π^- , K^+ , K^- , p , and \bar{p}) in deep inelastic scattering has been studied by the HERMES experiment. Using the 27.5 GeV positron beam at DESY, the hadron multiplicity from ^{14}N and ^{84}Kr has been measured and compared to that from deuterium. Significant nuclear effects have been observed suggesting a modification of the quark fragmentation process in nuclei.

1. Introduction

In the deep inelastic scattering (DIS) process, the production of hadrons can be viewed as the interaction of a virtual photon with a quark in the target nucleon (or nucleus) and the subsequent hadronization of that quark. Assuming these two processes are independent, the cross section can be written as a product of the quark distribution function, $q(x)$, and the fragmentation function, $D(z)$, weighted by the quark charge squared (e_f^2),

$$\sigma \sim \sum_f e_f^2 q_f(x) D_f^h(z). \quad (1)$$

The quark distribution function in the above equation describes the probability to find a quark with flavor f and a fraction x ($x = Q^2/2m\nu$) of the nucleon momentum, while the fragmentation function describes the probability of that quark to form a hadron of type h with a fraction z ($z = E_h/\nu$) of the energy of the virtual photon.

The formation of hadrons in deep inelastic scattering can be modified in the nuclear environment. In the simplest picture, the struck quark propagates a certain distance before forming a hadron. Either the quark or hadron may interact with the additional hadrons in the nucleus. Whether the quark-hadron or hadron-hadron interactions dominate will depend on the hadron formation time τ_f .

Nuclear effects in deep inelastic hadron production can be studied via the multiplicity ratio, R_M^h . This ratio measures the number of hadrons (of type h) per inclusive DIS event produced from a target with mass A compared to the hadron production rate from deuterium,

$$R_M^h(z, \nu) = \frac{\left(\frac{1}{\sigma} \frac{d\sigma}{dzd\nu}\right)_A}{\left(\frac{1}{\sigma} \frac{d\sigma}{dzd\nu}\right)_D} = \frac{\left(\frac{1}{N_e} \frac{dN_h}{dzd\nu}\right)_A}{\left(\frac{1}{N_e} \frac{dN_h}{dzd\nu}\right)_D}, \quad (2)$$

where N_e is the number of inclusive electrons and $dN_h/dzd\nu$ is the number of hadrons of type h in a given ν and z bin. The DIS normalized semi-inclusive yield for a particular target can be written in terms of fragmentation functions and quark distribution functions,

$$\frac{1}{N_e} \frac{dN_h}{dzd\nu} = \frac{\sum_f e_f^2 q_f(x) D_f^h(z)}{\sum_f e_f^2 q_f(x)}. \quad (3)$$

Hence, the multiplicity ratio defined in Eq. 2 is sensitive to potential modifications to the fragmentation process in nuclei.

2. Models of Hadron Attenuation in Nuclei

Below we will discuss a few of the models that have been used to describe attenuation in the deep inelastic production of hadrons.

2.1. Early Models

The one and two time-scale models are perhaps the most intuitive descriptions of hadron attenuation in nuclei. The one time-scale model assumes that the struck quark propagates for a mean time τ_f before the formation of the hadron [1]. In this model, the formation time is proportional to the energy of the created hadron and the multiplicity ratio is given by,

$$R_M^h = 2\pi \int_0^\infty b db \int_{-\infty}^\infty dl \rho_A(b, l) [P_A(b, l)]^{A-1}, \quad (4)$$

where ρ_A is the nuclear density and P_A is the probability to have no interaction as the quark and/or hadron propagates in the nucleus. This probability involves the quark-hadron cross section, σ_q , and the hadron-hadron cross section, σ_h . It is assumed that $\sigma_q \ll \sigma_h$ while $\sigma_h \approx 20$ mb. Hence, this model really only involves one degree of freedom, the hadron formation time, τ_f .

The two time-scale model extends the one time-scale model by assuming that the struck quark does not necessarily form the final hadron directly, but may instead form some quasi-hadron in an intermediate state [2]. In this model τ_f still describes the total formation time, *i.e.* the time between the hard interaction with the struck quark and formation of the final hadron, however an additional time, τ_c describes the time between the hard interaction and the formation of the intermediate hadronic state. Additionally, one must introduce the pre-hadron cross section, σ^* , which describes interactions between the quasi-hadronic intermediate state and the hadrons in the nucleus.

2.2. Gluon Bremsstrahlung

The gluon bremsstrahlung description of hadron attenuation in nuclei assumes that the final hadron is formed when the struck quark combines with a q or \bar{q} formed from a radiated gluon [3]. Large z hadrons retain much of the energy of the struck quark – hence, in the case where gluon bremsstrahlung is significant, the number of high z hadrons will be reduced. In this model the emission of gluons is enhanced in the nuclear environment, leading to a suppression at high z of the multiplicity ratio. In contrast to

the one and two time-scale models, hadron scattering in the final state is not significant in the gluon bremsstrahlung model due to color transparency effects.

2.3. Parton Multiple Scattering

The hadron multiplicity in nuclei may also be affected by parton multiple scattering. In this case, the fragmentation function is modified via quark rescattering with partons in other nucleons [4,5]. The dominant contribution comes from terms involving gluon radiation from the struck quark combined with rescattering from gluons from another parton. In this model, the modified fragmentation function, \tilde{D} , can be approximately written,

$$\tilde{D}_f^h(z) = D_f^h(z) + \Delta D_f^h(z), \quad (5)$$

where D_f^h is the unmodified fragmentation function and ΔD_f^h contains the modifications due to parton rescattering.

In Ref. [4], the modified fragmentation functions are calculated using higher twist parton distributions. These higher twist terms depend on diagonal and off-diagonal twist-four parton distributions, which in turn can be constrained using Drell-Yan pA data.

In this multiple scattering model, the size of the modification to the fragmentation function is proportional to $A^{2/3}$ and is larger at small x . This model makes specific predictions for the mean energy loss of quarks (*i.e.* a modification to z) in the nuclear medium, and also predicts a broadening of the transverse momentum (p_t) spectra of the produced hadrons.

3. Hadron Multiplicity Measurements at HERMES

The HERMES experiment has measured the hadron multiplicity ratio, R_M^h , from ^{14}N and ^{84}Kr . Positrons of 27.5 GeV in the HERA storage ring at DESY were incident on gas targets (nuclear and deuterium) while the scattered positrons and produced hadrons were detected in the HERMES spectrometer. The HERMES spectrometer consists of several sets of wire chambers for tracking, with a TRD, calorimeter, and

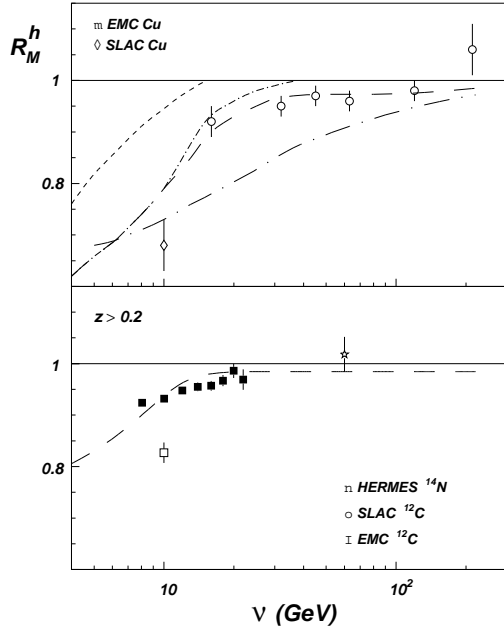


Figure 1. Charged hadron multiplicity ratio vs. ν ($z > 0.2$) for HERMES ^{14}N data and data from other experiments. The long-dashed curve is a two time-scale calculation with $\sigma_q = 0.75$ mb, $\sigma_h = \sigma^* = 20$ mb, and $\tau_h \propto (1 - \ln(z))E_h$.

Cerenkov detector for particle identification [6]. Prior to 1998, a threshold gas Čerenkov was used, allowing the separation of pions from other hadrons for $4 \text{ GeV} < p_\pi < 13.5 \text{ GeV}$. In 1998, a dual radiator ring imaging Čerenkov detector (RICH) was installed, allowing clean identification of pions, kaons, and protons separately over a momentum range of $2.5 \text{ GeV} < p < 15 \text{ GeV}$ (for pions and kaons) or $4 \text{ GeV} < p < 15 \text{ GeV}$ (for protons and antiprotons).

The data were analyzed as follows. Scattered positrons with $Q^2 > 1 \text{ GeV}^2$ and $W > 2 \text{ GeV}$ were selected to ensure that the kinematics of the process were in the deep inelastic regime and to avoid the nucleon resonance region. A further constraint of $y = \nu/E < 0.85$ was used to avoid having to apply large radiative corrections. The produced (charged) hadrons were identified either as a whole or separated by species as noted above. Hadrons from target fragmentation were

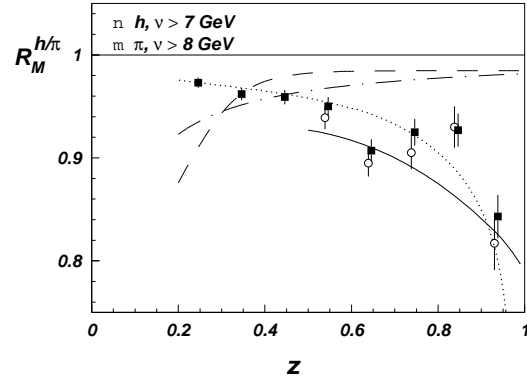


Figure 2. Multiplicity ratios for all charged hadrons (closed squares) and charged pions (open circles) as a function of z . The solid line is a gluon bremsstrahlung calculation while the other curves are one (dashed-dotted and dotted lines) and two (long-dashed line) time-scale calculations.

suppressed by requiring $z > 0.2$. Since ν and z are partially correlated in the HERMES acceptance, this z constraint, combined with the minimum hadron momentum constraints noted above implies $\nu > 7 \text{ GeV}$.

Figure 1 shows the multiplicity ratio for ^{14}N as a function of ν for all charged hadrons with $z > 0.2$ [7]. Also shown are data from SLAC [8] and CERN [9] for Cu (top panel) and ^{12}C (bottom panel). The dashed-dot curve is a one time-scale calculation while the other curves are two time-scale calculations for various values of σ^*

Table 1

Parameters for one and two time-scale model calculations shown in Figs. 1 and 2. The cross sections, σ_q , σ^* , and σ_h are given in mb and are described in Section 2.1. The model constants, c_h and κ , are $1 \text{ fm}/(\text{GeV}c)$ and $1 \text{ GeV}/\text{fm}$ respectively.

curve	τ_f (fm/c)	σ_q	σ^*	σ_h
.....	$c_h z \nu$	0	N/A	20
-----	$(1 - \ln(z))z\nu/(\kappa c)$	0.75	20	20
-	$(1 - \ln(z))z\nu/(\kappa c)$	0	20	20
-----	$(1 - \ln(z))z\nu/(\kappa c)$	0	0	20
.....	$c_h(1 - z)\nu$	0	N/A	20

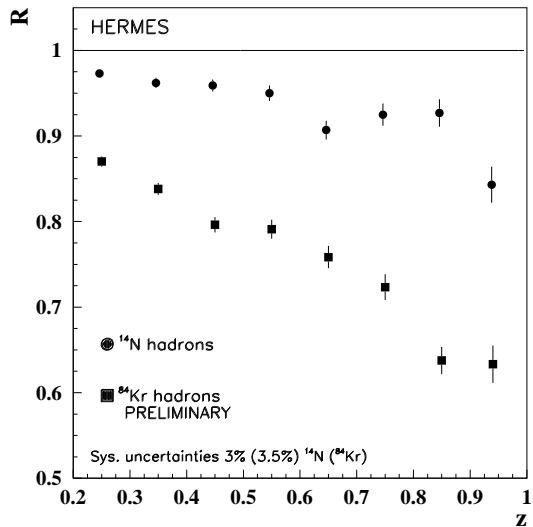


Figure 3. Multiplicity ratios for all charged hadrons ($\nu > 7$ GeV) for ^{14}N (circles) and ^{84}Kr (squares) as a function of z .

(note that $\sigma^* = \sigma_h$ is equivalent to a one time-scale calculation, although with a different definition of τ_f). The details of each calculation are listed in Table 1. Clearly, when examining the ν dependence and without differentiating between hadron types, these simple models can fit the data well.

The z dependence of the multiplicity ratio, however, reveals the weaknesses in the one and two time-scale models. Fig. 2 shows the z dependence of the HERMES ^{14}N multiplicity ratio for all hadrons and pions [7]. The solid curve is a gluon bremsstrahlung calculation for pions and agrees with the trend of the data rather well. It is interesting to note that the two time-scale model calculation with $\sigma^* = \sigma_h$ (long-dashed curve) which agreed well with the ν dependence seen in Fig. 1 does not give the correct z dependence. However, by using an ad-hoc expression for the formation time, $\tau_f \propto (1-z)\nu$, the correct z dependence can be recovered.

Newer HERMES data on ^{84}Kr allows one to examine the mass dependence of these effects. Fig. 3 show the multiplicity ratios for ^{84}Kr and ^{14}N as

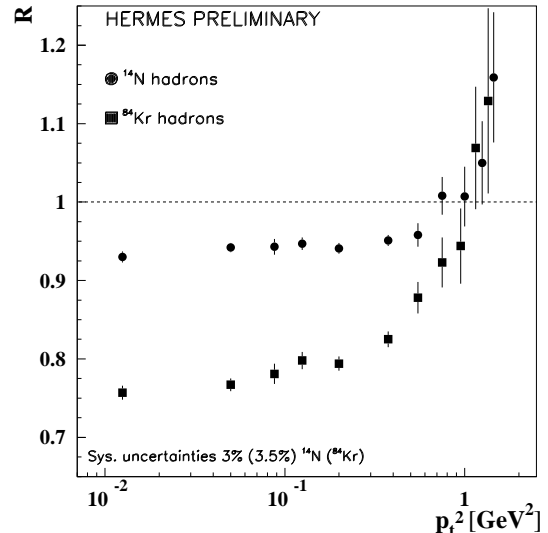


Figure 4. Multiplicity ratios for all charged hadrons ($\nu > 7$ GeV) for ^{14}N (circles) and ^{84}Kr (squares) as a function of p_t^2 .

a function of z . Clearly, the reduction in hadron multiplicity seen in the ^{14}N data is even larger in ^{84}Kr . This increase in the attenuation ($1 - R_A$) at large z is consistent with the parton multiple scattering predictions of Guo and Wang [4]. Furthermore, their prediction that the attenuation should increase quadratically with the nuclear size (i.e. $\propto A^{2/3}$) is consistent with the \approx factor of 3 increase in the attenuation in ^{84}Kr as compared to ^{14}N .

The transverse momentum (p_t) dependence of the HERMES multiplicity ratios is also consistent with the idea of parton multiple scattering leading to modification of the fragmentation functions. An enhancement of hadron multiplicities in proton-nucleus and nucleus-nucleus collisions (the so-called Cronin effect) has been explained in terms of parton multiple scattering [10] and a similar effect should apply in semi-inclusive lepton nucleus scattering [11]. The p_t^2 dependence of the multiplicity ratios is shown in Fig. 4 where an enhancement of the ratio at ≈ 1 GeV² is clearly evident for both the ^{14}N and ^{84}Kr data.

Finally, it should be noted that with the ex-

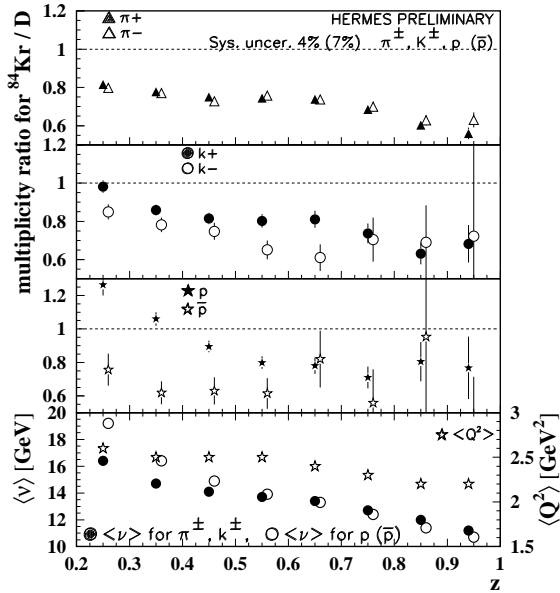


Figure 5. Multiplicity ratio as a function of z for π^\pm , K^\pm , protons and anti-protons. Also shown are the mean Q^2 and ν for each z bin (bottom panel).

cellent hadron identification capabilities of the RICH, the HERMES experiment has also been able to measure the multiplicity ratios for several types of particles *separately*. These results (available only for the ^{84}Kr data as the RICH was not yet installed during the ^{14}N data taking) are shown in Fig. 5. This data set will serve to further constrain models of semi-inclusive hadron production in nuclei. In particular, the different hadron-hadron cross sections ($\sigma_{\pi/K} \approx 20$ mb while $\sigma_{p/\bar{p}} \approx 40 - 60$ mb) will help disentangle fragmentation function modification effects from hadron rescattering effects. In fact, recent calculations [12] for π^\pm and K^\pm that incorporate both fragmentation function modifications and nuclear absorption show very good agreement with the HERMES ^{84}Kr data.

4. Considerations for Neutrino Scattering Experiments

Neutrino experiments in general rely heavily on detailed Monte Carlos to simulate the response of the rather complicated targets/detectors involved. These simulations are greatly enhanced by accurate descriptions of the nuclear effects involved.

In the context of low energy (few GeV) neutrino experiments, one is not so much concerned with the physics of hadron attenuation in semi-inclusive DIS as the effects on particle rates. Furthermore, it is likely that one need not model these effects with a great deal of precision. While the large energy spread of neutrino beams will ensure that deep inelastic scattering ($Q^2 > 1 \text{ GeV}^2$, $W > 2 \text{ GeV}$) will play some role, it will certainly not be the dominant process.

The majority of semi-inclusive hadrons produced in DIS are pions, so one need not worry about the different attenuation ratios for the different species of hadrons. It is also likely not necessary to include the p_t dependence of the hadron attenuation ratio since most of the effect observed is at rather large p_t , which is only a small part of the total phase space involved. That said, a good first step in taking hadron attenuation effect into account is likely the one time-scale parameterization ($\tau_f \propto (1-z)\nu$) shown in Fig. 2 (dotted line). The A dependence could then be taken into account via a simple $A^{2/3}$ scaling in $1 - R_A$.

5. Acknowledgements

This work was supported by DOE Contract N. DE-AC05-84ER40150 under which the Southeastern Universities Research Association (SURA) operates the Thomas Jefferson National Accelerator Facility (Jefferson Lab) and by DOE Contract N. DE-FG03-95ER40913 under which the Nuclear Physics Laboratory at the University of Colorado operates.

REFERENCES

1. A. Bialas and T. Chmaj, Phys. Lett. B **133**, 241 (1983).

2. A. Bialas and M. Gyulassy, Nucl. Phys. B **291**, 793 (1987).
3. B. Kopeliovich, J. Nemchik and E. Predazzi, arXiv:hep-ph/9511214.
4. X. F. Guo and X. N. Wang, Phys. Rev. Lett. **85**, 3591 (2000)
5. X. N. Wang and X. F. Guo, Nucl. Phys. A **696**, 788 (2001).
6. K. Ackerstaff *et al.* [HERMES Collaboration], Nucl. Instrum. Meth. A **417**, 230 (1998).
7. A. Airapetian *et al.* [HERMES Collaboration], Eur. Phys. J. C **20**, 479 (2001).
8. L. S. Osborne *et al.*, Phys. Rev. Lett. **40**, 1624 (1978).
9. J. Ashman *et al.* [European Muon Collaboration], Z. Phys. C **52**, 1 (1991).
10. E. Wang and X. N. Wang, Phys. Rev. C **64**, 034901 (2001).
11. X. Guo and J. Qiu, Phys. Rev. D **61**, 096003 (2000).
12. A. Accardi, V. Muccifora and H. J. Pirner, Nucl. Phys. A **720**, 131 (2003).